

Electronic Supporting Information

**Acceptor Engineering of Small Molecule Fluorophores for NIR-II
Fluorescent and NIR-I Photoacoustic Imaging**

Yaxi Li,^{‡a} Hongli Zhou,^{‡b} Renzhe Bi,^c Xiuting Li,^c Yanqing Yang,^b Jen-Shyang Ni,^a Weng Heng Liew,^d Malini Olivo,^c Kui Yao,^d Jie Liu,^{*b} Hao Chen,^{*e} Kai Li^{*a}

a. Shenzhen Key Laboratory of Smart Healthcare Engineering, Department of Biomedical Engineering, Southern University of Science and Technology, Shenzhen, Guangdong 518055, China. E-mail: lik@sustech.edu.cn

b. Key Laboratory of Flexible Electronics (KLOFE) Institute of Advanced Materials (IAM), Nanjing Tech University (Nanjing Tech), 30 South Puzhu Road, Nanjing 211800, China. E-mail: iamjieliu@njtech.edu.cn

*c. Institute of Bioengineering and Bioimaging (IBB), A*STAR (Agency for Science, Technology and Research), 11 Biopolis Way, Singapore*

*d. Institute of Materials Research and Engineering, A*STAR (Agency for Science, Technology and Research), 2 Fusionopolis Way, Innovis, 138634, Singapore*

e. Center for Molecular Imaging Research, Shanghai Institute of Materia Medica, Chinese Academy of Sciences, Shanghai, 201203, China. E-mail: haoc@simm.ac.cn

Experimental section

Materials

DSPE-PEG-OCH₃ and DSPE-PEG-Maleimide are commercial products from Laysan Bio, Inc. Dichloromethane (DCM), dimethyl sulfoxide (DMSO), and tetrahydrofuran (THF) were purchased from Sigma-Aldrich. Dulbecco's modified eagle medium (DMEM), fetal bovine serum (FBS), and penicillin-streptomycin were provided by Thermo Fisher Scientific. All other chemicals were purchased from Sigma-Aldrich or Energy Chemical (China) and used as received. 1-(4-Bromophenyl)-2,2-bis(4-methoxyphenyl)-1-phenylethene **1** was prepared according to the previous report.¹

Synthesis of 1-(4-Bromophenyl)-2,2-bis(4-hydroxyphenyl)-1-phenylethene (**2**)

To a solution of 1,1-bis(4-methoxy)phenyl-2-(4-bromophenyl)-2-phenylethene **1** (1.41 g, 3 mmol) in anhydrous dichloromethane (40 mL) at -78 °C under argon atmosphere was slowly added BBr₃ (9 mL, 1 M in dichloromethane, 9 mmol). Then the reaction mixture was kept at this temperature for 2 h, followed by stirring at room temperature for 20 h. After quenching the reaction with ice water, the reaction mixture was sequentially extracted with dichloromethane (40 mL × 3), washed with water (100 mL × 3), dried over Na₂SO₄, and filtered. After removing the organic solvent, the residue was purified by silica gel column chromatography (chloromethane/methane = 99/1) to give a white-like solid (1.19 g, yield: 90%). ¹H NMR (400 MHz, CD₃OD) δ: 7.23–7.20 (m, 2 H), 7.13–7.05 (m, 3 H), 6.98–6.95 (m, 2 H), 6.88–6.78 (m, 6 H), 6.57–6.49 (m, 4 H), 4.57 (br, 2 H). ¹³C NMR (100 MHz, CD₃OD) δ: 157.14, 157.02, 145.28, 144.99, 142.89, 138.52, 136.23, 136.19, 134.20, 133.67, 133.62, 132.34, 131.73, 128.79, 127.20, 120.71, 115.61, 115.43.

Synthesis of 1-(4-Bromophenyl)-2,2-bis(4-octyloxyphenyl)-1-phenylethene (**3**)

To a mixture of **2** (1.11 g, 2.5 mmol), Cs₂CO₃ (2.43 g, 7.5 mmol) in anhydrous *N,N*-dimethylformamide (DMF, 15 mL) under argon atmosphere was added 1-bromooctane (1.25 g, 6.5 mmol). The reaction mixture was allowed to stir at room temperature for 12 h. Then the reaction mixture was poured in to water (50 mL), and sequentially extracted with dichloromethane (30 mL × 3), washed with water (100 mL × 5), dried over MgSO₄, and filtered. After solvent removal under reduced pressure, the residue was purified by silica gel column chromatography (petroleum ether/dichloromethane = 9/1) to afford compound **3** as viscous liquid (1.51 g, yield: 91%). ¹H NMR (400 MHz, CDCl₃) δ: 7.21 (m, 2 H), 7.11–7.07 (m, 3 H), 7.00 (m, 2 H), 6.92–6.87 (m, 6 H), 6.65–6.59 (m, 4 H), 3.87 (m, 4 H), 1.73 (m, 4 H), 1.43 (m, 4 H), 1.30 (m, 16 H), 0.88 (m, 6 H). ¹³C NMR (100 MHz, CDCl₃) δ: 157.91, 157.82, 143.91, 143.43, 141.00, 137.68, 135.84, 135.76, 133.08, 132.56, 132.53, 131.38, 130.85, 127.81, 126.25, 119.96, 113.74, 113.57, 67.89, 67.84, 31.84, 29.42, 29.40, 29.34, 39.33, 29.26, 26.10, 26.09, 22.68, 14.13.

Synthesis of 2-(4-(2,2-bis(4-(octyloxy)phenyl)-1-phenylvinyl)phenyl)thiophene (**4**)

A schlenk tube was charged with **3** (1.33 g, 2 mmol), 2-(tributylstannyl)thiophene (1.49 g, 4 mmol), Pd₂(dba)₃ (55 mg, 0.06 mmol), P(*o*-tolyl)₃ (36 mg, 0.12 mmol) and toluene (20 mL). After the mixture was kept at 100 °C for 24 h under argon atmosphere, the reaction was quenched with water (100 mL). The mixture was sequentially extracted with dichloromethane (50 mL × 3), washed with water (100 mL × 3), dried over MgSO₄, and filtered. After solvent removal, the residue was purified by silica gel column chromatography (petroleum ether/dichloromethane = 7/3) to afford compound **4** as viscous liquid (1.16 g, yield: 87%). ¹H NMR (400 MHz, CDCl₃) δ: ¹H NMR (400 MHz, CDCl₃) δ: 7.37 (d, *J* = 8 Hz, 2 H), 7.25–7.22 (m, 2 H), 7.12–7.09 (m, 3 H), 7.06–7.01 (m, 5 H), 6.98–6.92 (dd, *J* = 8 Hz, 16 Hz, 4 H), 6.69–6.61 (m, 4 H), 3.90–3.86 (m, 4 H), 1.77–1.71 (m, 4 H), 1.44–1.41 (m, 4 H), 1.35–1.28 (m, 16 H), 0.91–0.87 (m, 6 H). ¹³C NMR (100 MHz, CDCl₃) δ: 157.80, 157.71, 144.42, 144.25, 143.75, 140.58, 138.40, 136.12, 132.62, 131.92, 131.86, 131.49, 127.97, 127.74, 125.04, 122.73, 113.66, 113.53, 67.85, 67.83, 31.85, 29.42, 29.35, 29.27, 26.10, 26.09, 22.70, 14.15.

Synthesis of 2-(4-(2,2-bis(4-(octyloxy)phenyl)-1-phenylvinyl)phenyl)-5-tributylstannylthiophene (**5**)

To a solution of **4** (671 mg, 1 mmol) in anhydrous THF (20 mL) at -78 °C was added *n*-BuLi (1 mL, 1.6 M) under argon atmosphere. The reaction mixture was kept at this temperature for 1.5 h, followed by the addition of tributyltin chloride (870 μL, 3 mmol) in one portion. Then it was allowed to stir at room temperature for 15 h. The mixture was poured into water (40 mL) and extracted with dichloromethane (30 mL × 3). The combined organic

phase was washed with water (50 mL × 3), dried over Na₂SO₄, and filtered. After solvent removal, the compound 5 was obtained as a liquid without purification for further use.

Synthesis of 4,8-Bis{4-[2,2-bis(4-octoxyphenyl)-1-phenylvinyl]phenyl}-6-(2-ethylhexyl)[1,2,5]thiadiazolo[3,4-f]benzotriazole (BTB)

The compound 5 (480 mg, 0.5 mmol), 4,8-dibromo-6-(2-ethylhexyl)-[1,2,5]thiadiazolo[3,4-f]benzotriazole (89.4 mg, 0.2 mmol), Pd₂(dba)₃ (18.3 mg, 0.02 mmol), P(*o*-tolyl)₃ (12.2 mg, 0.04 mmol) and toluene (20 mL) were placed in a Schlenk tube and heated to 100 °C for 20 h under argon atmosphere. The reaction mixture was extracted with dichloromethane (50 mL × 3), washed with water (100 mL × 3), dried over MgSO₄, and filtered. After removing the solvent under reduced pressure, the residue was purified by silica gel column chromatography (petroleum ether/dichloromethane = 6/4) to afford BTB as a green solid (208 mg, yield: 64%). ¹H NMR (400 MHz, CDCl₃) δ: 8.81 (d, *J* = 4 Hz, 2 H), 7.55 (d, *J* = 8 Hz, 4 H), 7.45 (s, 2 H), 7.12–6.93 (m, 22 H), 6.69–6.62 (m, 8 H), 3.89 (s, 8 H), 2.39–2.01 (m, 2 H), 1.74 (m, 8 H), 1.54–1.29 (m, 45 H), 1.05 (m, 4 H), 0.90 (m, 18 H). ¹³C NMR (100 MHz, CDCl₃) δ: 158.07, 157.92, 150.04, 147.84, 144.41, 144.31, 142.64, 140.93, 138.66, 136.85, 136.29, 132.80, 132.44, 132.14, 131.69, 127.92, 126.31, 125.15, 123.96, 113.90, 113.73, 111.75, 68.02, 31.95, 30.88, 29.84, 29.52, 29.37, 26.23, 23.11, 22.79, 14.22, 10.82. MADLI-TOF-MS *m/z* [M] Calcd for C₁₀₆H₁₂₃N₅O₄S₃, 1626.877; found, 1627.207.

Synthesis of 4,8-Bis{4-[2,2-bis(4-octoxyphenyl)-1-phenylvinyl]phenyl}benzo[1,2-*c*:4,5-*c'*]bis[1,2,5]thiadiazole (BBT)

BBT was obtained as black solid (72 mg, yield: 47%) using a similar synthetic procedure as BTB, starting from compound 5 (480 mg, 0.5 mmol), 4,8-dibromobenzo[1,2-*c*:4,5-*c'*]bis[1,2,5]thiadiazole (70.4 mg, 0.2 mmol), Pd₂(dba)₃ (18.3 mg, 0.02 mmol), P(*o*-tolyl)₃ (12.2 mg, 0.04 mmol) in toluene (20 mL). ¹H NMR (400 MHz, CDCl₃) δ: 8.93 (d, *J* = 4 Hz, 2 H), 7.54 (d, *J* = 8 Hz, 4 H), 7.44 (d, *J* = 4 Hz, 2 H), 7.16–7.07 (m, 14 H), 7.01 (d, *J* = 4 Hz, 2 H), 6.69 (d, *J* = 8 Hz, 4 H), 6.64 (d, *J* = 4 Hz, 4 H), 3.89 (m, 8 H), 1.77–1.71 (m, 8 H), 1.46–1.38 (m, 8 H), 1.32–1.25 (m, 32 H), 0.90 (m, 6 H), 0.85 (m, 6 H). ¹³C NMR (100 MHz, CDCl₃) δ: 158.13, 157.96, 151.11, 149.30, 144.73, 144.35, 141.10, 138.63, 137.40, 136.27, 134.11, 132.82, 132.21, 131.84, 131.70, 131.00, 128.96, 127.96, 126.36, 125.26, 124.19, 113.94, 113.74, 113.14, 68.04, 31.97, 31.93, 29.85, 29.54, 29.50, 29.38, 29.36, 26.23, 22.81, 22.77, 14.24, 14.20. MADLI-TOF-MS *m/z* [M] Calcd for C₉₈H₁₀₆N₄O₄S₄, 1531.713; found, 1530.754.

Synthesis of BTB-RGD NPs

The BTB NPs were synthesized through a modified nanoprecipitation method as we reported before. In brief, BTB (1 mg) and DSPE-PEG-OCH₃ (2 mg) were mixed and dissolved in 1 mL of THF. The THF solution was quickly injected into 9 mL of DI water, followed by sonication using a probe sonicator for 90 seconds. The solution was dialyzed against DI water for 2 days and then concentrated using an Amicon Ultra-4 centrifugal filter unit (MWCO 10kDa) and filtered through a 0.2 μm syringe filter. To afford BTB-RGD NPs, a mixture of DSPE-PEG-OCH₃ (1 mg) and DSPE-PEG-RGD (1 mg) was used as the encapsulation matrix. The obtained BTB NPs and BTB-RGD NPs were stored at 4 °C for further use.

Characterization

Nuclear magnetic resonance (NMR) spectra were recorded on a Bruker Avance III 400 MHz NMR spectrometer (400 MHz for ¹H, referenced to TMS at δ = 0.00 ppm and 100 MHz for ¹³C, referenced to CDCl₃ at 77.0 ppm). The hydrodynamic diameter and zeta potential were measured on Micromeritics Nanoplus-3 (US). Transmission electron microscopy (TEM) images were obtained on a JEOL JEM-2100 electron microscope with an accelerating voltage of 200 KV. UV-vis-NIR spectra were measured on a Shimadzu UV-1750 spectrometer. Photoluminescence (PL) spectra were recorded on an Edinburgh instruments FLS980, using Xe lamp as the excitation source and a liquid nitrogen cooled InGaAs diode detector for signal detection. Fluorescence quantum yield was determined using IR26 in 1,2-dichloroethane (0.5%) as the standard. The absorbance of solutions was controlled below 0.1 to avoid the internal filter effect. The average particle size of NPs was determined by a Zetasizer Nano ZS equipment at room temperature.

Determination of photothermal conversion efficiency

BTB NP or BBT NP solutions (200 μL) with BTB concentrations of 50 and 100 μg mL⁻¹ were added in each well of a 96-well plate. A continuous-wave diode laser of 730 nm or 808 nm (diode-pumped solid-state laser) was used to irradiate each well at a laser intensity of 1 W cm⁻², respectively. The temperature change of the solution was recorded in a real-time manner with a FLIR thermal imaging system. The photothermal conversion efficiency was then calculated according to the published literature.²

Photoacoustic signal measurement

The performance of BTB NPs was first evaluated through *in vitro* measurement using a commercial PA imaging equipment, MSOT EIP 10 (iTheraMedical, Germany). The NP suspensions with different concentrations (7.81, 31.25, 62.5, and 125 $\mu\text{g mL}^{-1}$ of BPTB) were filled into polyethylene tubes individually. The sample-filled tube was placed in a water tank at a depth corresponding to the transducer's focus. Another tube filled with pure DI water was placed by side as a control to compensate for the variations during different runs for signal processing. Images were recorded under pulse laser excitation from 660 to 950 nm at an interval of 5 nm with a repetition rate of 10 Hz. The data were then extracted by the integrated software to generate PA spectra.

To evaluate the tissue penetration depth of BTB NPs in PA imaging, the sample-filled polyethylene tube (BTB concentration of 62.5 $\mu\text{g mL}^{-1}$) was covered by chicken tissues with a thickness of 0, 2, 4, 8, 10, 12 mm, respectively. The PA spectrum of the sample under chicken tissues with different thickness was then recorded using MSOT EIP 10 with pulsed laser excitation from 660 to 950 nm at an interval of 5 nm with a repetition rate of 10 Hz.

In vitro cytotoxicity of BTB NPs

The *in vitro* cytotoxicity of BTB NPs was studied by CellTiter[®] 96 AQueous One Solution Cell Proliferation Assay. Mouse NIH/3T3 fibroblast was purchased from American Type Culture Collection (ATCC). Dulbecco's modified eagle medium supplemented with 10% of fetal bovine serum and 1% of penicillin-streptomycin was used as the culture medium of the cells. To evaluate the cytotoxicity of BTB NPs, the NIH/3T3 cells were seeded in a 96-well plate at a concentration of 5,000 cells/well. After 24 h incubation, the medium was discarded and BTB NPs suspended in fresh medium at varying concentrations ([BTB] = 2.5, 5, 10, 20, 40, and 80 $\mu\text{g mL}^{-1}$) was added to each well for 72 h incubation at 37 °C. The cells without treatment of BTB NPs were used as a control group. CellTiter[®] 96 AQueous One Solution reagent (20 μL) was added into each well and the absorbance at 490 nm was recorded after 2 h incubation. The metabolic viability of cells treated with different BTB concentrations was calculated based on the ratio of the absorbance of treated cells to that of untreated cells.

Cellular uptake of the non-functionalized and RGD-functionalized nanoprob

To investigate the targeting efficiency to tumor cells, the cells were first cultured in confocal chambers or six-well plates to achieve 80% confluence, respectively. The cells were then co-cultured with 40 $\mu\text{g mL}^{-1}$ of BTB NPs or BTB-RGD NPs for 4 h, respectively. After washing with 1 \times PBS buffer (pH = 7.2-7.4) to eliminate the free NPs, the cells in confocal chambers were fixed by 4% paraformaldehyde *via* a confocal laser scanning microscopy (Olympus, FV3000) for fluorescence imaging (Excitation: 730 nm; Filter: 760-890 nm).

Animal study

All animal experiments were performed in compliance with guidelines set by the Institutional Animal Care and Use Committee (IACUC) of Southern University of Science and Technology, Biological Resource Center, and Stanford Animal Research Committee.

NIR-II fluorescent microscopy imaging

A Nikon ECLIPSE Ni fluorescent microscope with an InGaAs camera (Princeton Instruments, NIRvana TE 640), 785 nm, 140 mW cm^{-2} laser excitation, 1000 nm long-pass filter (Thorlabs) was used for NIR-II fluorescent microscopy imaging. To evaluate the tissue penetration depth of BTB NPs in FL imaging, the NP suspensions with different concentrations (7.81, 31.25, 62.5, and 125 $\mu\text{g mL}^{-1}$) were added in each well of a 96-well plate individually. Next, the three parallel sample in 96-well plate (BTB concentration of 62.5 $\mu\text{g mL}^{-1}$) was covered by chicken tissues with a thickness of 0, 2, 4, 8, 10, 12 mm, respectively.

In vivo toxicity of BTB NPs

The *in vivo* cytotoxicity of BTB NPs was evaluated by a mouse model. C57BL/6 mice were purchased from InVivos. BTB NPs (100 $\mu\text{g}/\text{mouse}$) in saline were injected through tail vein. After 7 days post injection, the mice were sacrificed to collect the heart, liver, spleen, lung, and kidneys. The organs were fixed by formalin solution (neutral buffered, 10%) and embedded in paraffin for sectioning. The sectioned tissues were processed for haematoxylin eosin (H&E) staining. Mice without administration of BTB NPs were used as a control group for comparison.

In vivo vasculature imaging using PAM

The near-infrared photoacoustic microscopy (NIR-PAM) imaging system is retrofitted based on a commercially available PAM system (MicroPhotoAcoustics, Inc., USA). A continuously wavelength-tuneable Ti:sapphire NIR pulsed laser (*Advanced Optowave Corporation*, USA) is used as the light source. The laser has an emission wavelength range from 700 nm to 900 nm with a pulse width of < 18 ns. The line width is ~2nm. The maximum repetition rate could reach 1 KHz with a maximum pulse energy of 1 mJ at 800 nm.

Mice that are 6-8-week-old were anaesthetized through intra-peritoneal injection of ketamine-xylazine (150 mg kg⁻¹ ketamine and 10 mg kg⁻¹ xylazine). A 30G injection needle was inserted into the tail vein and glued on the skin. The syringe was filled with saline. Then the mouse was moved to a stage with a constant temperature controller on the top. The temperature was set at 37 °C. A small amount of ultrasound gel was applied to the imaging area without any air bubble. Finally, the imaging stage was moved underneath the water tank.

The emission wavelength was tuned at 730 nm with a pulse energy of 100 μJ. The first scan was performed without NP injection. After the pre-injection scanning, the BTB NP solution in saline (50 μg) was injected through the tail vein. The post-injection scanning was performed after 5, 15, 30, and 45 mins afterwards.

Photoacoustic Imaging (PAI) of tumor-bearing mice

The photoacoustic signals were recorded using a Nexus 128 photoacoustic instrument (Endra Inc., Boston, MA) with a series of laser wavelengths in the range of 680-950 nm using a continuous rotation mode (with a scan time of 12 s per wavelength, 240 views, 1 pulse/view). The spatial resolution of PA imaging is limited to be 280 μm. The PA data is reconstructed in volumes of 256 × 256 × 256 with 0.1 × 0.1 × 0.1 mm voxels. The system is equipped with a tunable nanosecond pulsed laser (7 ns pulses, 20-Hz pulse repetition frequency, wavelength-dependent laser power density, about 4–7 mJ/pulse on the animal surface) and 128 unfocused ultrasound transducers (with 5 MHz center frequency and 3 mm diameter) arranged in a hemispherical bowl filled with water (temperature is set to 38 °C). The imaging data were analyzed using Amide's a Medical Image Data Examiner (AMIDE) and Osirix software (Pixmeo SARL, Bernex, Switzerland).

Tumor-bearing mice (n=3 per group, 48h post *iv* injection of BTB-RGD or BTB NPs) were anesthetized with 2% isoflurane in oxygen was placed in the imaging tray at an appropriate position within the focal field of view (20 mm diameter sphere). The PA signals within the FOV were recorded, and the average voxel intensities within the regions of interest (ROIs) were quantitatively analyzed using AMIDE or Osirix. Supporting video 1: PAT imaging of 143B tumor with BTB-RGD NPs 48h post injection. Supporting video 2: PAT imaging of 143B tumor with BTB NPs 48h post injection.

Notes and references

- 1 X. Qin, H. Chen, H. Yang, H. Wu, X. Zhao, H. Wang, T. Chour, E. Neofytou, D. Ding, H. Daldrup-link, S. C. Heilshorn, K. Li, and J. C. Wu, *Adv. Funct. Mater.* 2018, **28**, 1704939.
- 2 (a) R. D. Keith, W. Ahn, and M. Hoepfner, *J. Phys. Chem. C*, 2007, **111**, 3636-3641. (b) Q. Tian, F. Jiang, R. Zou, Q. Liu, Z. Chen, M. Zhu, S. Yang, J. Wang, J. Wang, and H. Hu, *ACS Nano*, 2011, **5**, 9761-9771.

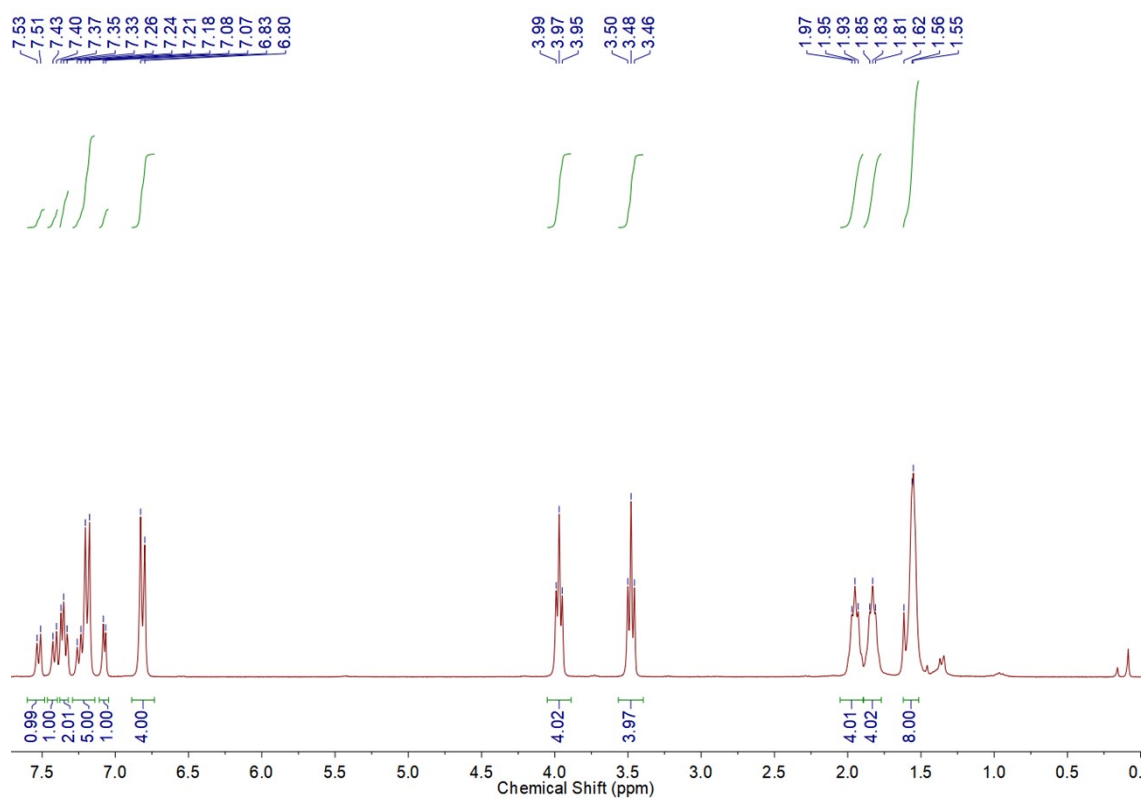


Figure S1. ^1H NMR spectrum of BTB in CDCl_3 .

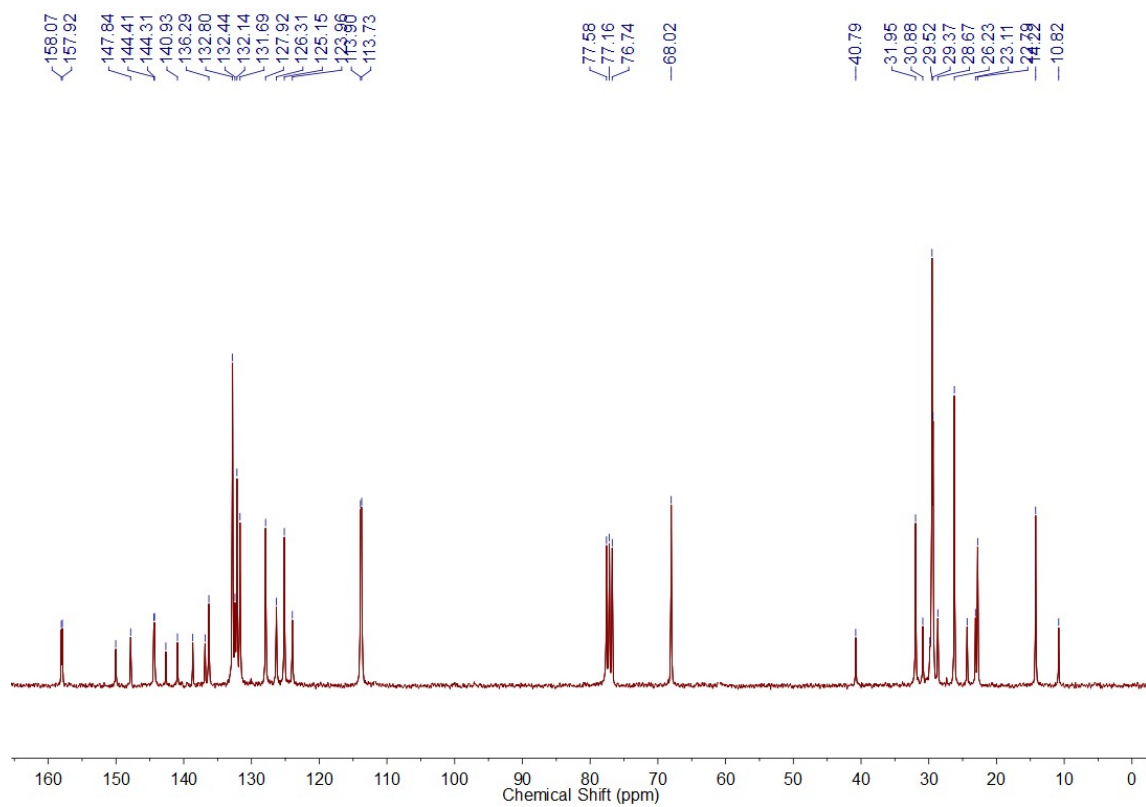


Figure S2. ^{13}C NMR spectrum of BTB in CDCl_3 .

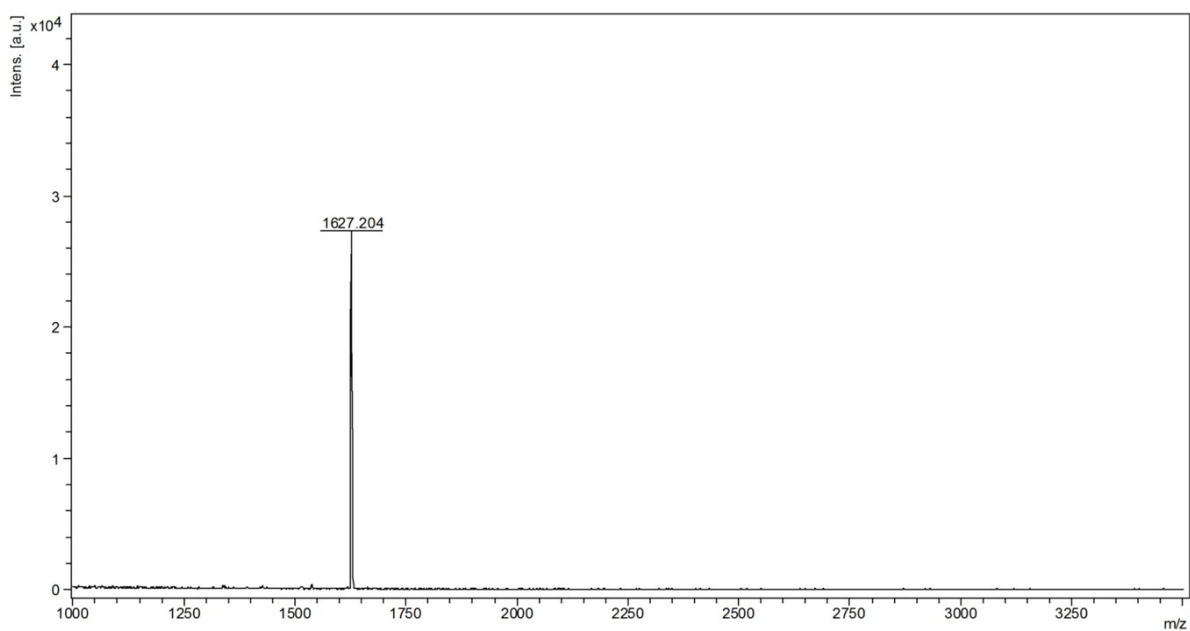


Figure S3. MALDI-TOF-MS measurement of BTB.

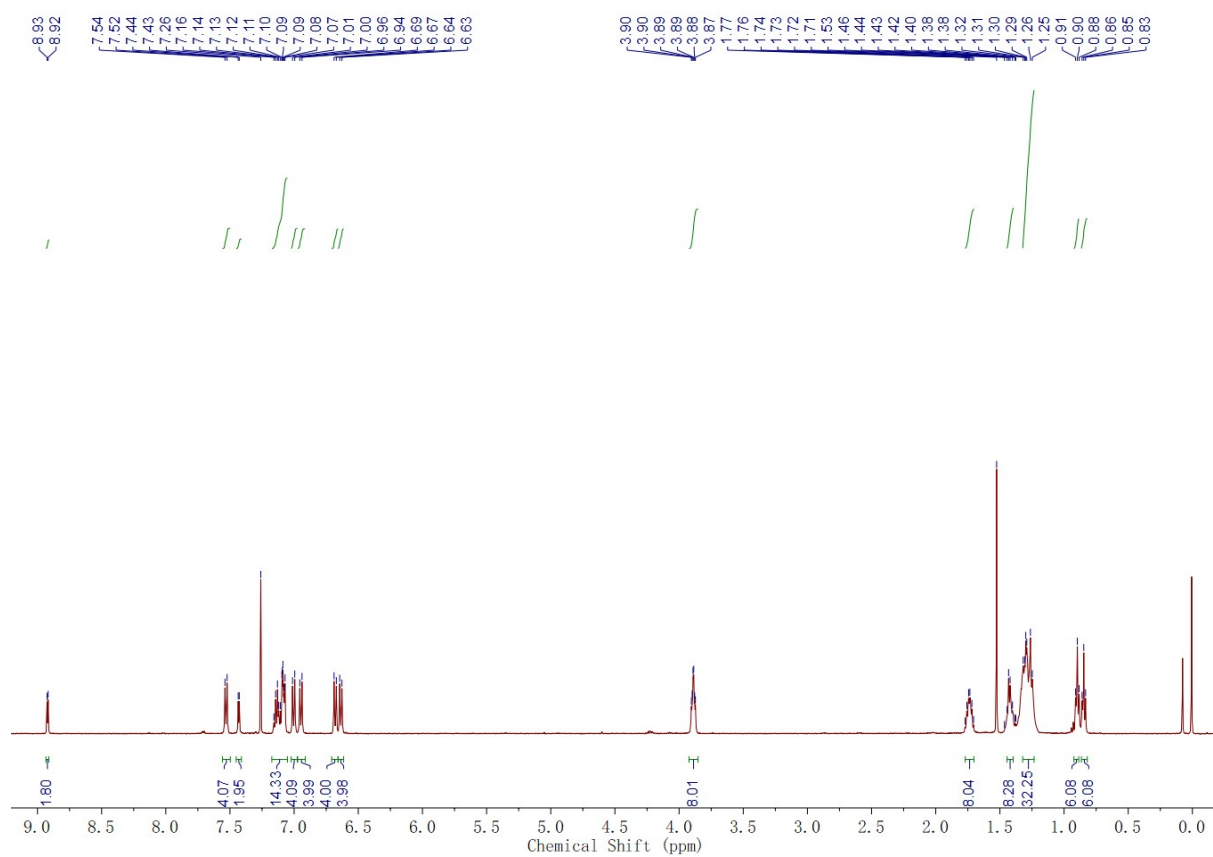


Figure S4. ¹H NMR spectrum of BBT in CDCl₃.

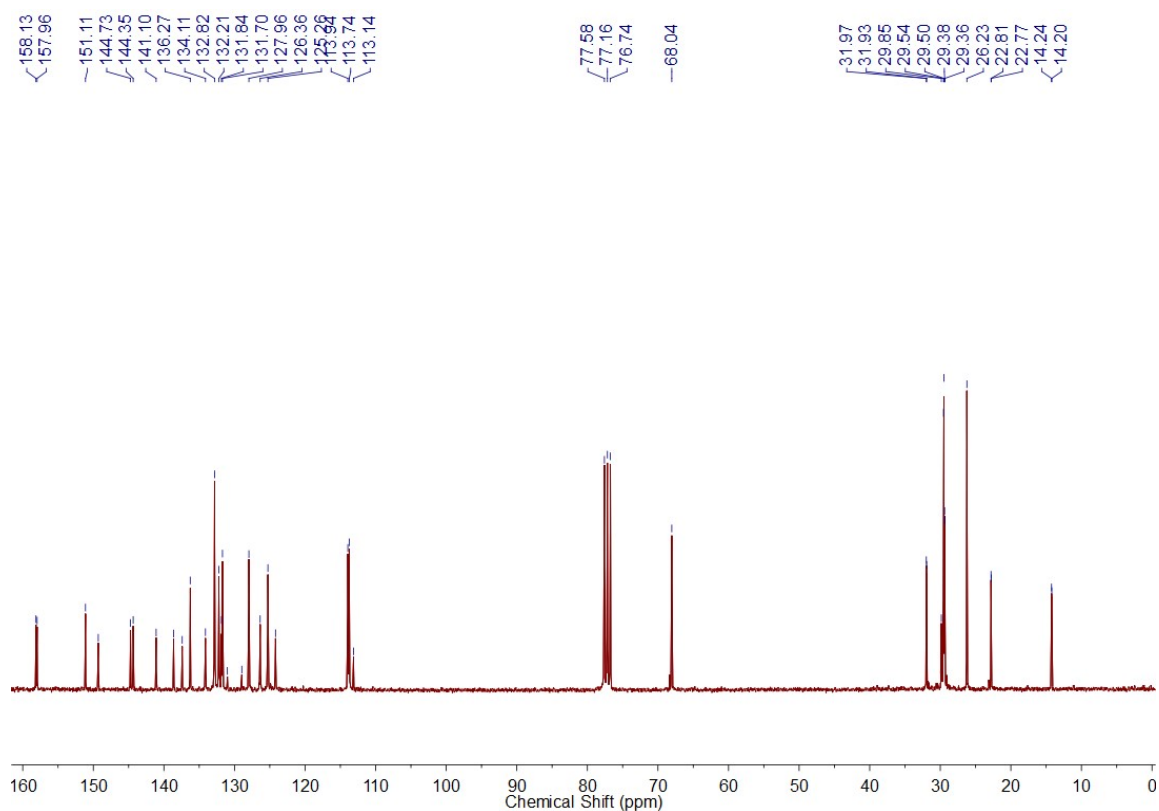


Figure S5. ^{13}C NMR spectrum of BBT in CDCl_3 .

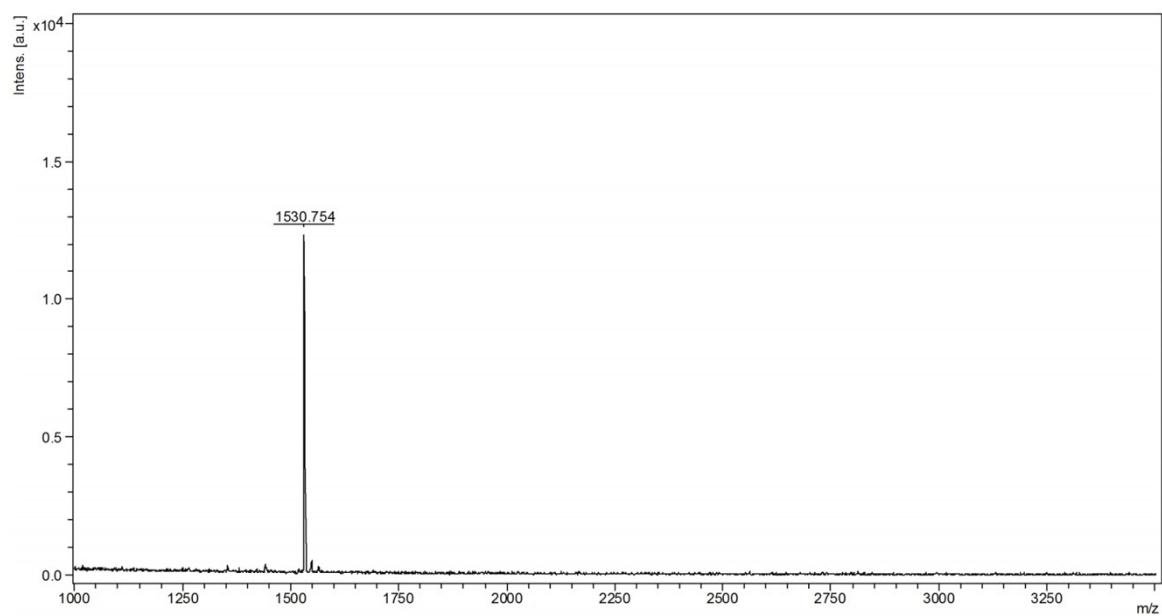


Figure S6. MALDI-TOF-MS measurement of BBT.

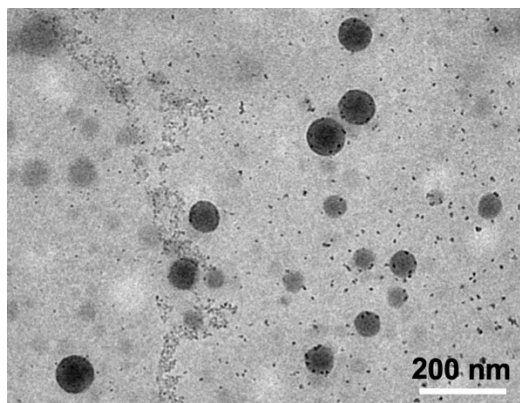


Figure S7. TEM images of BBT NPs.

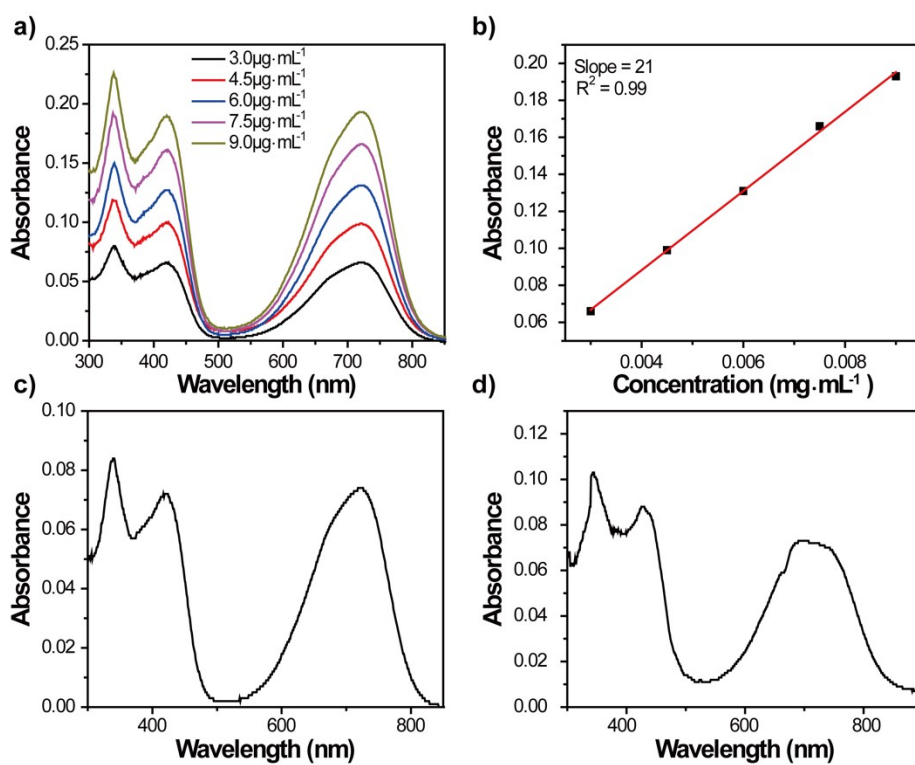


Figure S8. (a) UV-vis-NIR spectra of BTB in CHCl₃ at different concentrations. (b) Mass extinction coefficient of BTB at 730 nm in chloroform. (c) UV-vis-NIR spectrum of BTB NPs in CHCl₃ after freeze-drying. (d) UV-vis-NIR spectrum of BTB NPs in water.

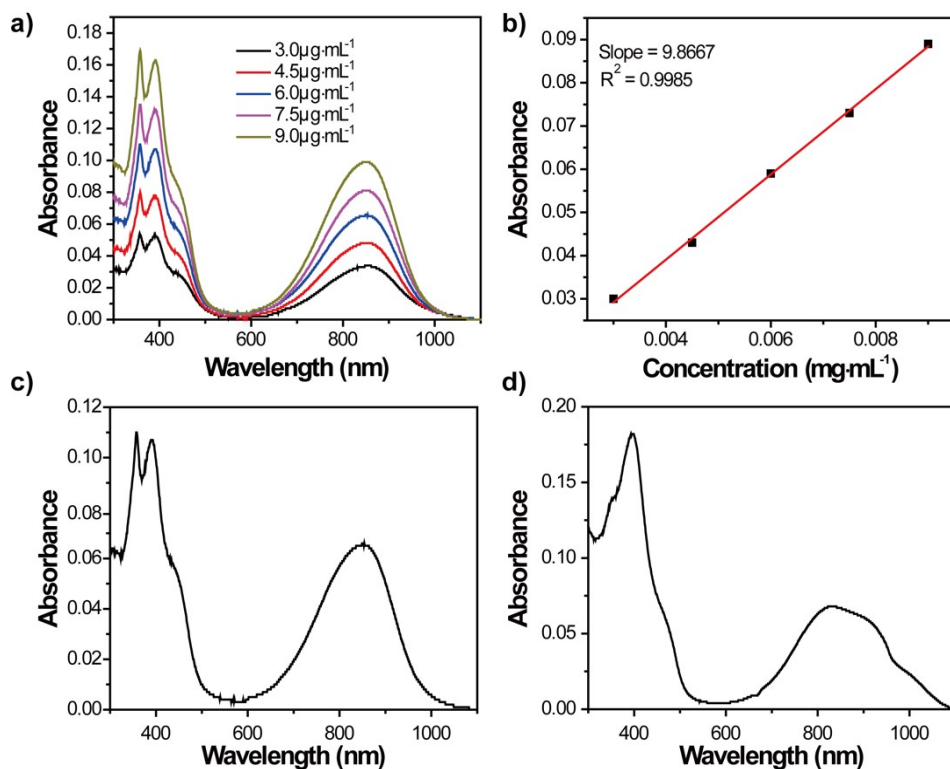


Figure S9. (a) UV-vis-NIR spectra of BBT in CHCl_3 at different concentrations. (b) Mass extinction coefficient of BBT at 808 nm. (c) UV-vis-NIR spectrum of BBT NPs in CHCl_3 after freeze-drying. (d) UV-vis-NIR spectrum of BBT NPs in water.

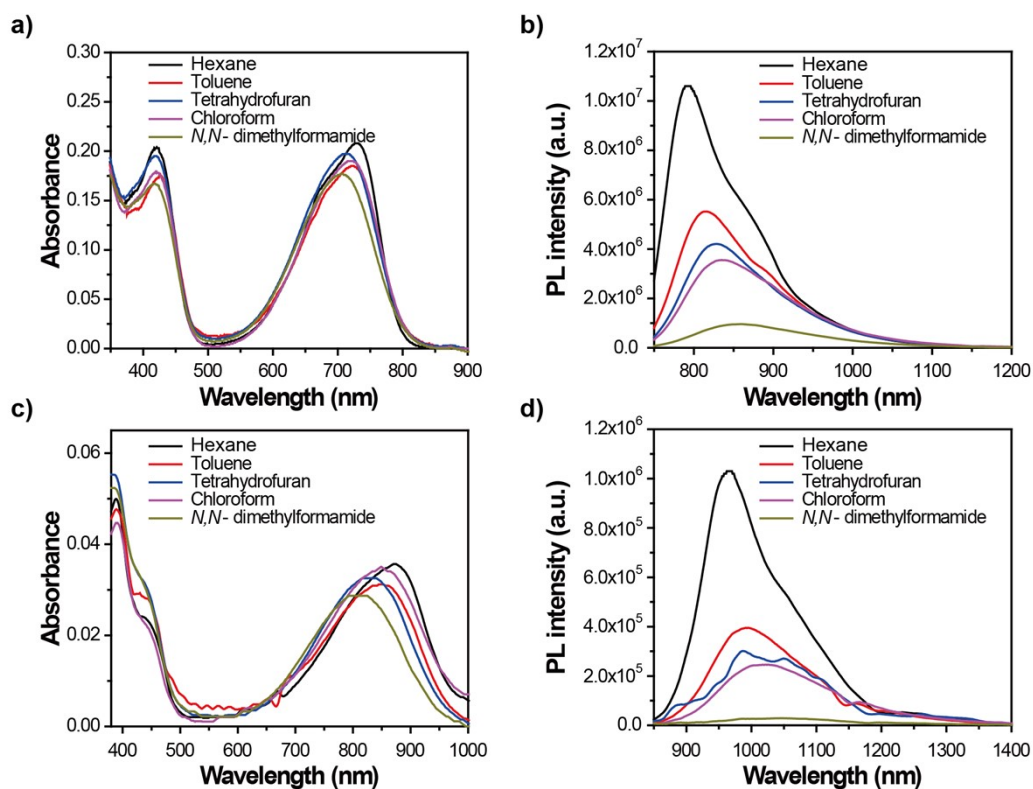


Figure S10. UV-vis-NIR and PL spectra of BTB and BBT in different organic solvents.

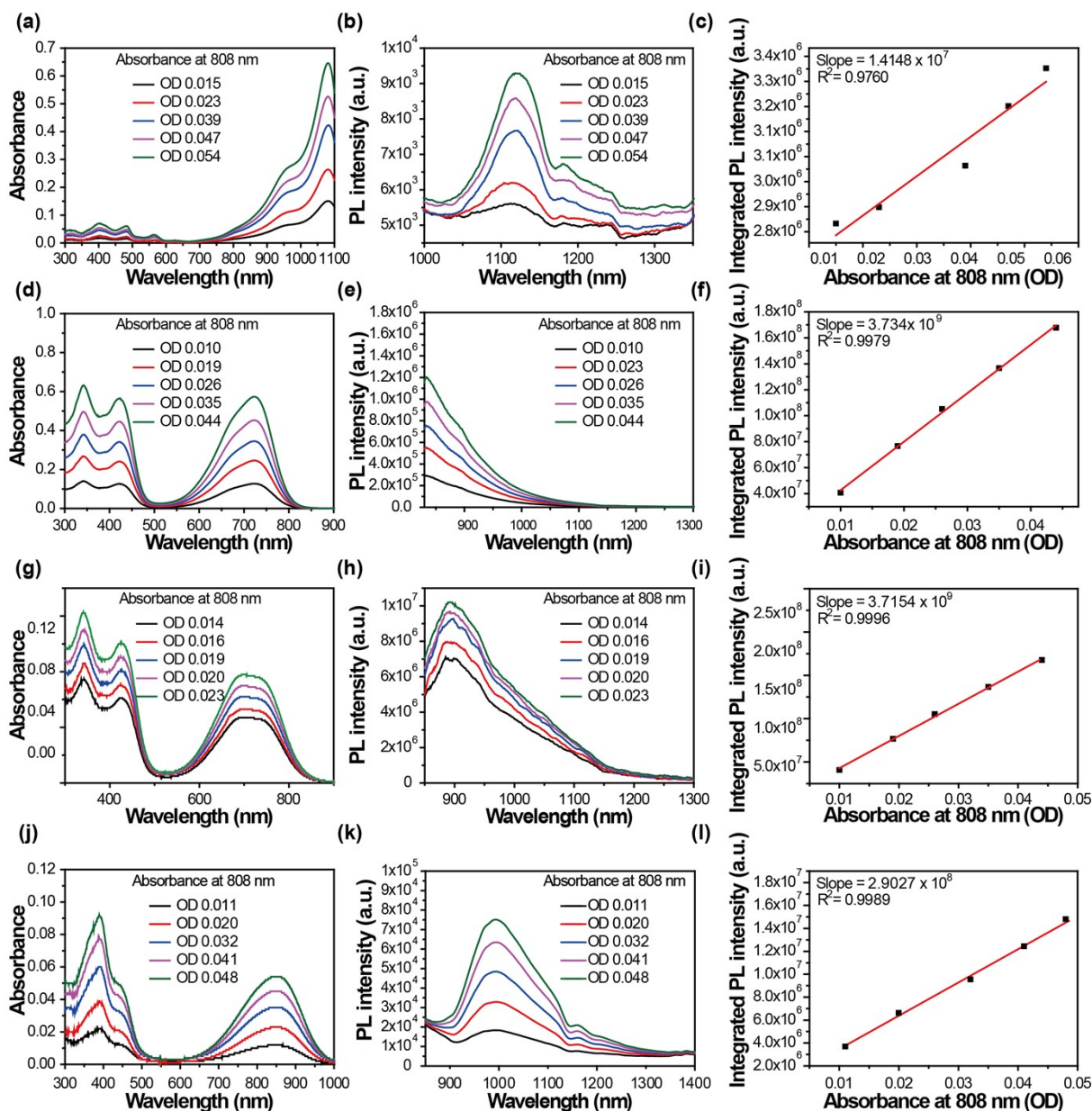


Figure S11. QY measurement of BTB NPs in aqueous solution, as well as BTB and BBT in toluene. a) UV-vis-NIR absorption spectra of IR26 in 1,2-dichloroethane with increasing concentrations. b) PL spectra of IR26 in 1,2-dichloroethane as shown in a) under an excitation of 808 nm. c) Integrated PL intensity plotted as a function of optical density (OD) at 808 nm for IR26 based on the measurements in a) and b); d) UV-vis-NIR absorption spectra of BTB in toluene with increasing concentrations. e) PL spectra of BTB as shown in d) under an excitation of 808 nm. f) Integrated PL intensity plotted as a function of optical density at 808 nm for BTB based on the measurements in d) and e). The QY of BTB in toluene was calculated to be 14.4%; g) UV-vis-NIR absorption spectra of BTB NPs in water with increasing concentrations. h) PL spectra of BTB NPs as shown in g) under an excitation of 808 nm. i) Integrated PL intensity plotted as a function of optical density at 808 nm for BTB NPs based on the measurements in g) and h). The QY of BTB NPs in water was calculated to be 0.48%; j) UV-vis-NIR absorption spectra of BBT in toluene with increasing concentrations. k) PL spectra of BBT as shown in j) under an excitation of 808 nm. l) Integrated PL intensity plotted as a function of optical density at 808 nm for BBT based on the measurements in j) and k). The QY of BBT in toluene was calculated to be 1.1%.

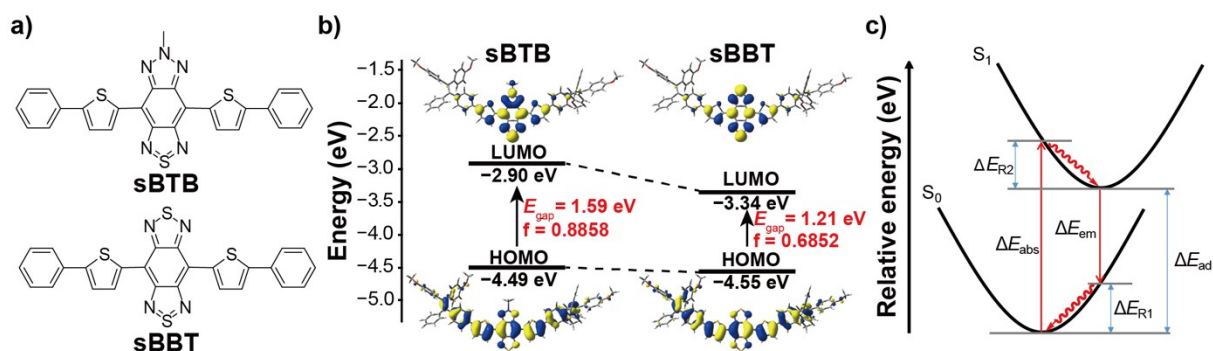


Figure S12. (a) Molecular structures of sBTB and sBBT. (b) Molecular orbitals, energy levels and geometries of sBBT and sBTB in ground state, calculated with TD-DFT as the level of B3LYP/6-31G*. (c) Electronic properties of sBTB and sBBT.

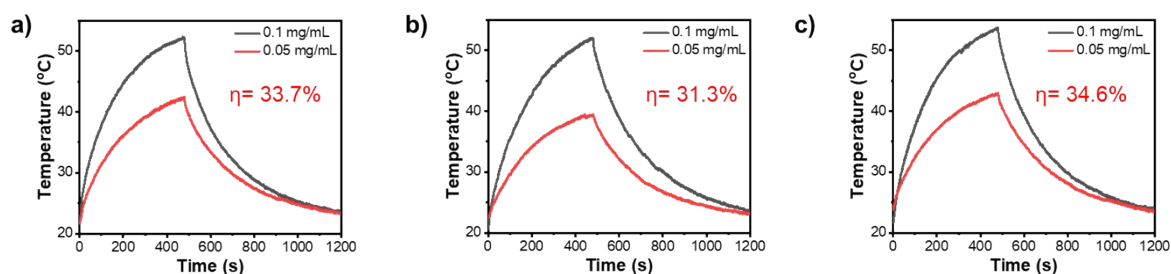


Figure S13. Determination of photothermal conversion efficiency of a) BTB NPs and b) BBT NPs under the excitation of a 730 nm laser at 1 W cm^{-2} , and c) BBT NPs under the excitation of an 808 nm laser at 1 W cm^{-2} . All NPs were tested in water solution.

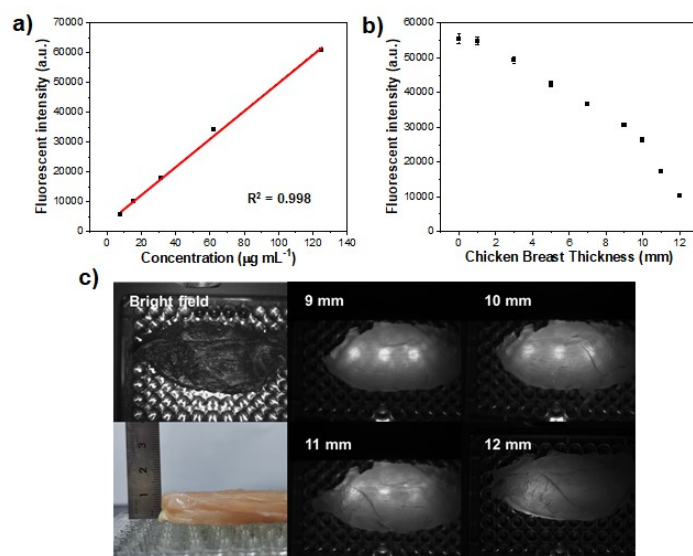


Figure S14. (a) The fluorescent signal intensity as a function of the concentration of BTB NPs upon excitation at 808 nm. (b) The change of fluorescent signal of BTB NPs ($62.5 \mu\text{g mL}^{-1}$) at different depth covered by chicken breast tissues upon excitation at 808 nm. (c) NIR-II FLI images of BTB NPs under different thickness of chicken tissues under 808 nm laser (1000 LP, 100 mW cm^{-2}).

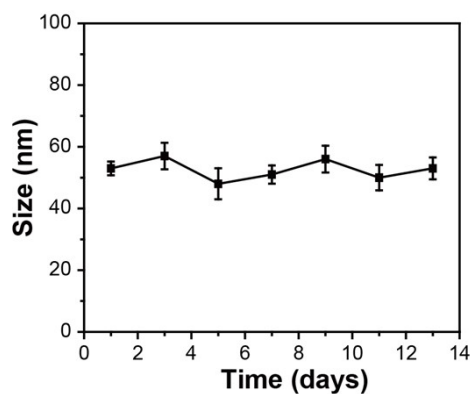


Figure S15. Size measurement of BTB NPs within two weeks using dynamic light scattering (DLS).

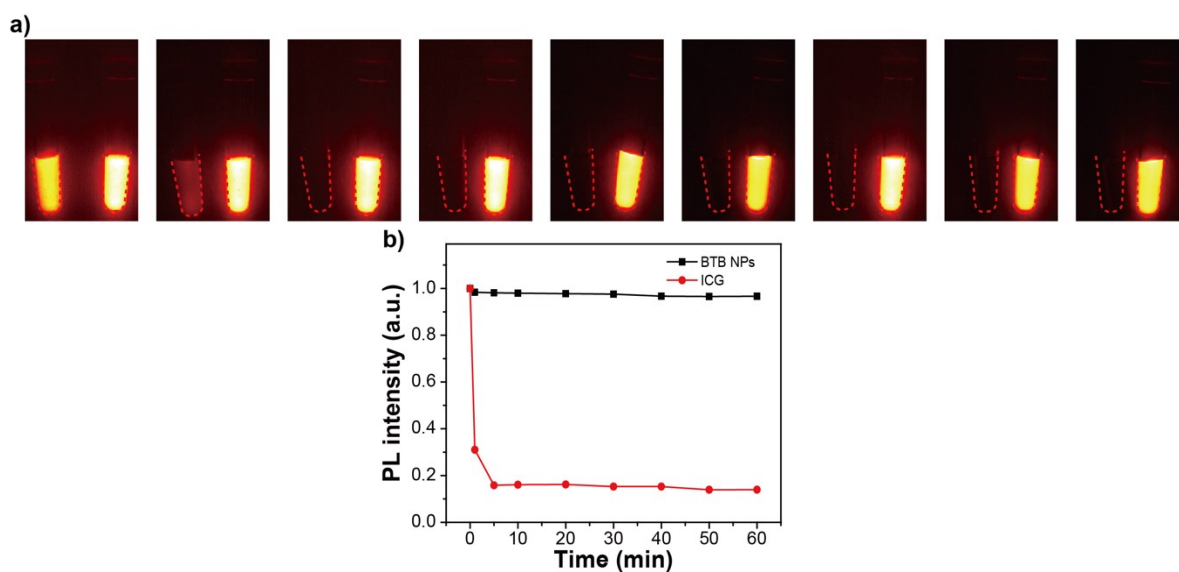


Figure S16. Fluorescence intensity changes of BTB NPs and ICG in water under continuous laser excitation (808 nm, 500 mW cm⁻²). Concentration: 0.05 mg mL⁻¹.

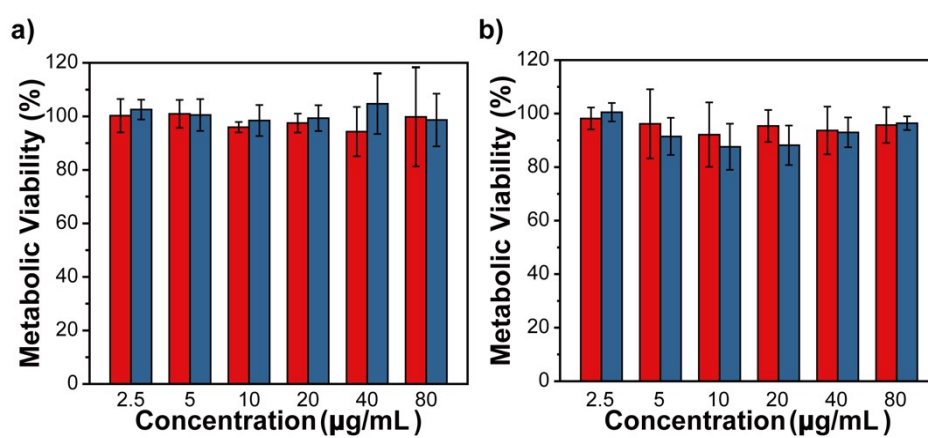


Figure S17. Cell viability of U87MG cells (a) and NIH/3T3 (b) after incubation with BTB NPs at different concentrations for 24 h.

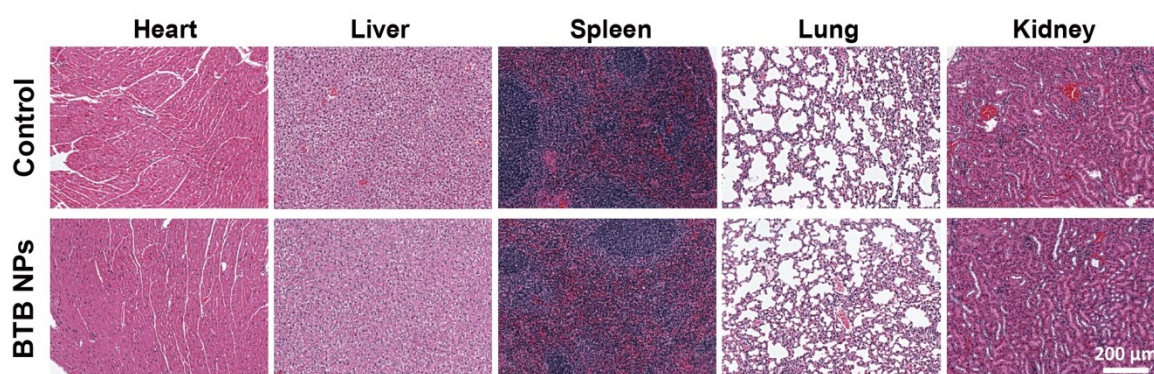


Figure S18. Pathological images (H&E staining) of important organs (heart, liver, spleen, kidney and lung).

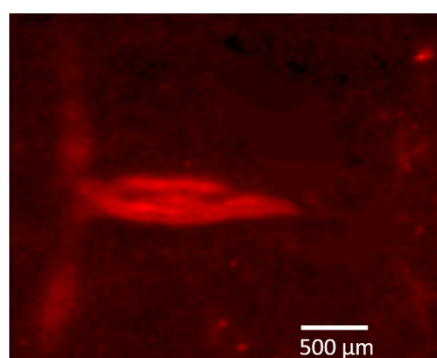


Figure S19. PAM imaging of mouse brain vessels before injection of BTB NPs.

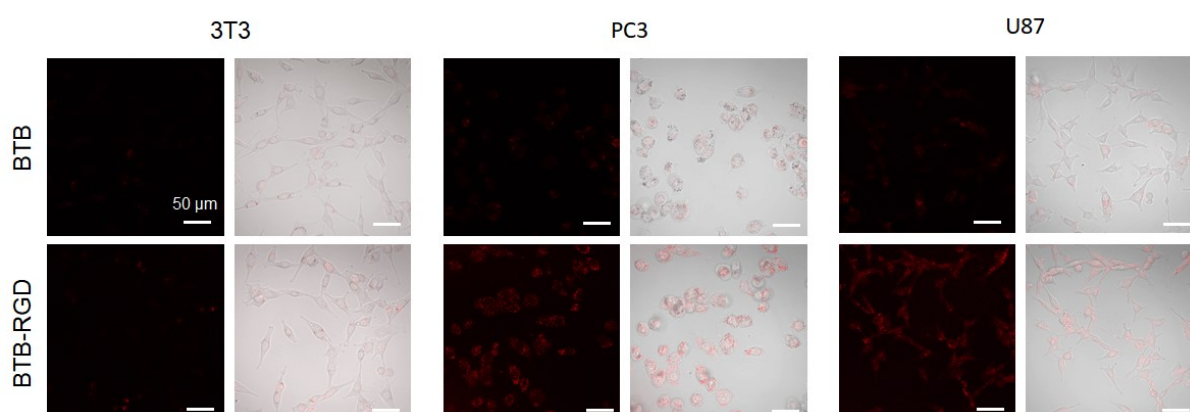


Figure S20. The confocal images of 3T3 cells, PC3 cells, and U87 cells treated with $40 \mu\text{g mL}^{-1}$ of BTB-RGD or BTB NPs for 4 hours (excitation: 730 nm; filter: 760-890 nm). Scale bar = 50 μm .

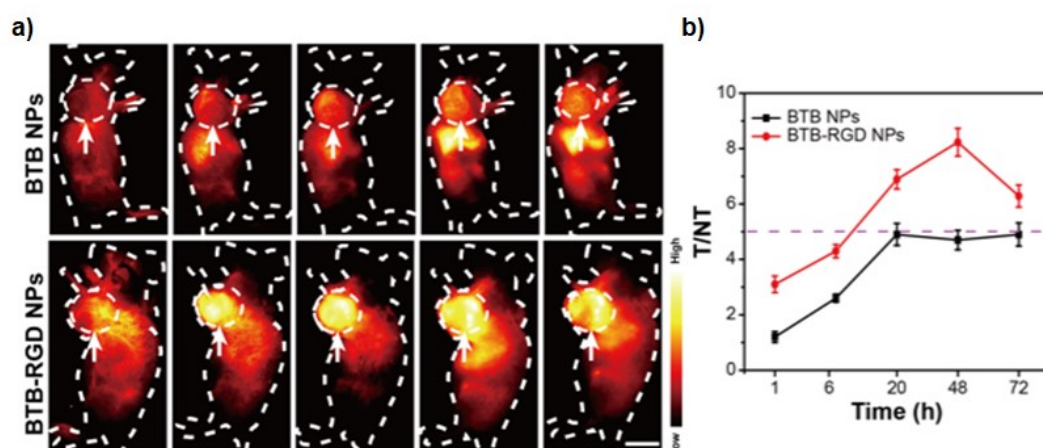


Figure S21. (a) Representative tumor imaging in PC3 tumor-bearing mice using BTB NPs over 72 h, under excitation by an 808 nm diode laser (140 mW cm^{-2}); images taken with a 1000 nm LP filter. Arrows indicate the subcutaneous PC3 tumor ($n = 4$ per group). (b) T/NT ratios in BTB NPs-based PC3 tumor imaging over 72 h. Data are plotted as mean \pm SD. $n = 4$, Scale bar: 5 mm.

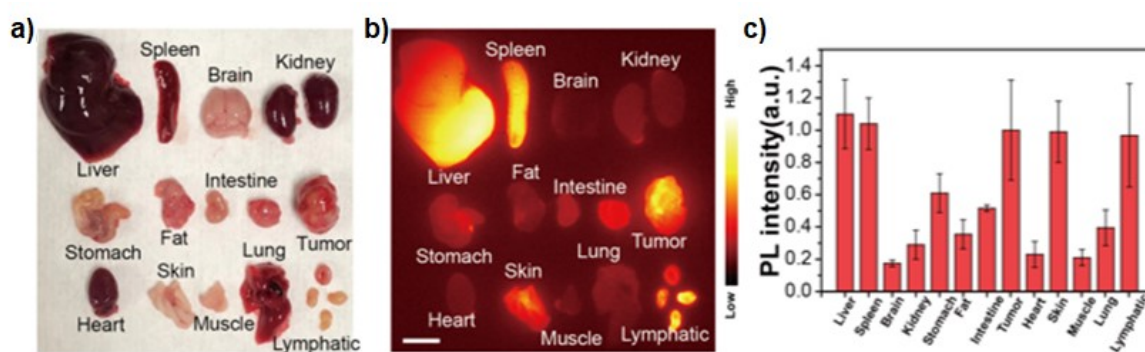


Figure S22. (a, b) Ex vivo biodistribution of BTB-cRGD NPs in the vital organs collected from a representative 143B tumor-bearing mouse at 72 h post injection, Scale bar: 5 mm. (c) Normalized mean fluorescence intensity of different organs.

Table S1. Theoretical calculation of electronic properties of sBTB and sBBT in solution.

Energy (eV)	sBTB	sBBT
ΔE_{abs}	1.59 eV	1.21 eV
ΔE_{em}	1.32 eV	0.99 eV
f_{S1}	0.45	0.30
k_r	$5.5 \times 10^{-11} \text{ s}^{-1}$	$2.1 \times 10^{-11} \text{ s}^{-1}$
ΔE_{R1}	0.13 eV	0.12 eV
ΔE_{R2}	0.13 eV	0.12 eV
ΔE_{ad}	1.45 eV	1.11 eV